Seasonal Flows on Warm Martian Slopes

Alfred S. McEwen *et al.*

Science **333**, 740 (2011);
DOI: 10.1126/science.1204816

Seasonal Flows on Warm Martian Slopes

Alfred S. McEwen,[1]* Lujendra Ojha,[1] Colin M. Dundas,[2] Sarah S. Mattson,[1] Shane Byrne,[1] James J. Wray,[3] Selby C. Cull,[4] Scott L. Murchie,[5] Nicolas Thomas,[6] Virginia C. Gulick[7]

Water probably flowed across ancient Mars, but whether it ever exists as a liquid on the surface today remains debatable. Recurring slope lineae (RSL) are narrow (0.5 to 5 meters), relatively dark markings on steep (25° to 40°) slopes; repeat images from the Mars Reconnaissance Orbiter High Resolution Imaging Science Experiment show them to appear and incrementally grow during warm seasons and fade in cold seasons. They extend downslope from bedrock outcrops, often associated with small channels, and hundreds of them form in some rare locations. RSL appear and lengthen in the late southern spring and summer from 48°S to 32°S latitudes favoring equator-facing slopes, which are times and places with peak surface temperatures from ~250 to 300 kelvin. Liquid brines near the surface might explain this activity, but the exact mechanism and source of water are not understood.

Although there is much morphological evidence for water flow on Mars in the past, little definitive evidence exists for surface water today. The chloride and sulfate minerals on Mars are indicative of widespread and abundant brines in Mars geologic history (*1*–*5*). Salts can depress the freezing point of water by up to 70 K and reduce the evaporation rate by factors of 10 or more, so brines would be far more stable than pure water at the surface of Mars (*2*, *6*–*10*). Here we describe observations by the High Resolution Imaging Science Experiment (HiRISE) (*11*) on the Mars Reconnaissance Orbiter (MRO) of features we call recurring slope lineae (RSL). RSL are narrow (0.5- to 5-m) markings, up to ~40% darker than their surroundings, on steep slopes (>25°; table S2); and they are recurring, forming and growing in warm seasons (late spring to early fall) and fading or vanishing in cold seasons. Confirmed RSL have been found to date at seven locations (Table 1), often with many separate clusters. There are 12 other likely RSL sites and 20 candidate sites. They extend downslope from bedrock outcrops or rocky areas and are often associated with small channels (Figs. 1 and 2 and figs. S3 to S5). RSL have lengths up to hundreds of meters, and more than 10^3 lineae may be present in a HiRISE observation. Along with several other hypotheses, we explore the potential of briny flows as a formation mechanism of RSL.

Our survey of HiRISE images of steep slopes [supporting online material (SOM)] has identified confirmed and likely RSL only in the southern hemisphere from 32°S to 48°S, favoring equator-facing slopes (table S1). There are also eight candidate RSL sites in equatorial regions (18°S to 19°N), but they are few in number at each site, and the seasonal recurrence has not been confirmed (table S3 and fig. S6). Where repeat imaging within a Mars year is available, RSL are observed to form and grow from late southern spring to early fall, and to fade or disappear in other seasons [L_S (the areocentric longitude of the Sun) = 20 to 245] (*12*) (figs. S1 and S2). RSL extend down the topographic gradient, diverting around obstacles rather than overtopping them. Individual lineae may split or merge. Because they terminate on steep slopes, RSL lengths must be controlled by a limited volume of mobile material.

There are up to five images per season for confirmed RSL sites, which show that they grow incrementally but not concurrently at uniform rates (SOM) (*13*). Some RSL may be unchanged between images (typically a few weeks or months apart in time), whereas others have lengthened by small or substantial amounts. Measured growth rates range from 0 to 20 m/day on average (fig. S3), but given sparse temporal coverage it could be as much as 560 m per event, with no other activity over several weeks.

RSL occur in the classical dark regions of Mars, which have moderate thermal inertias (~200 to 340 J m^{-2} $s^{-1/2}$ K^{-1}) (table S3); the bedrock outcrops probably have much higher thermal inertias. Determining the composition of RSL from orbit is challenging, as they are much smaller than the ~18 m–per–pixel scale of MRO's Compact Reconnaissance Imaging Spectrometer for Mars (CRISM) (*14*). RSL cover a substantial fraction of resolvable slopes in some areas (Figs. 1 and 2), but no distinctive spectral features have been identified, including the strong absorption features expected from even small quantities of water. Hydrated minerals are associated with bedrock at several RSL sites, such as phyllosilicates in Asimov Crater and chlorite, kaolinite, and hydrated silica in the central structure of Horowitz Crater (*15*), but there is no known correlation between RSL regions and particular minerals (SOM).

Slopes containing RSL are steep, near the angle of repose for cohesionless particles (table S2), and appear to be sites of active mass wasting (no superimposed aeolian bedforms). Numerous small channels (1 to 50 m wide) often cover these slopes, but RSL are rarely associated with the larger Martian gullies (ravines). RSL are found in only ~1% as many HiRISE images as are gullies. In a few cases (Fig. 1 and figs. S3 to S5), the presence and lengths of RSL are so similar to those of the fine channels that a genetic association seems likely, although cause and effect are not clear. Topographic changes associated with RSL have not been observed.

Other Martian slope features may appear similar to RSL. The seasonal, latitudinal, and slope aspect distribution of RSL and their occurrence in regions with a low dust index distinguish them from slope streaks (*16*) (Table 2). Small slope lineaments are also seen on high-latitude dunes and in a few non-dune gully alcoves during late winter and spring, as the seasonal CO_2 cover is sublimating. Although it has been proposed that the dune streaks are due to brines (*17*), the alternate hypothesis of sand flows initiated by CO_2 sublimation has been confirmed by the appearance of new dune gullies (*18*). Other dry mass-wasting features may resemble RSL, but lack seasonal recurrence.

Table 1. RSL types.

RSL type	Description and seasonal behaviors	Number of sites	Latitude range	Number of RSL per site
Confirmed RSL	Observed to recur in multiple warm seasons and fade in cold seasons	7	48°S to 32°S	10^2 to 10^3
Likely RSL	Evidence for fading in cold seasons, but not yet observed to recur in multiple years	12	47°S to 34°S	10 to 10^3
Candidate equatorial RSL	Morphology and geologic setting of RSL, changes observed, but seasonality unclear	8	18°S to 19°N	10 to 10^2
Candidate RSL poleward of 30°S	Morphology and geologic setting of RSL, but no repeat imaging	12	52°S to 31°S	10 to 10^3

[1]Lunar and Planetary Laboratory, University of Arizona, Tucson, AZ 85721, USA. [2]U.S. Geological Survey, Flagstaff, AZ 86001, USA. [3]Department of Astronomy, Cornell University, Ithaca, NY 14853, USA. [4]Department of Earth and Planetary Sciences, Washington University, St. Louis, MO 63130, USA. [5]Johns Hopkins University Applied Physics Laboratory, Laurel, MD 20723, USA. [6]Physikalisches Institut, University of Bern, Bern, Switzerland. [7]NASA Ames Research Center and SETI Institute, Moffett Field, CA 94035, USA.

*To whom correspondence should be addressed. E-mail: mcewen@lpl.arizona.edu

The seasonal, latitudinal, and slope aspect distributions show that RSL require relatively warm temperatures. Summertime afternoon brightness temperatures measured from orbit (*19*) on RSL-covered slopes in the middle to late afternoon range from 250 to 300 K, with daily peak temperatures probably being higher (table S1). Equatorial regions reach temperatures comparable to warm-season temperatures on equator-facing slopes in the southern mid-latitudes. Northern summers are cooler because perihelion occurs shortly before the northern winter solstice. In spite of the equatorial candidates, RSL are clearly most abundant in the southern mid-latitudes.

A range of hypotheses must be considered to explain these observations. Thermal cycling can damage rocks (*20*) and might eventually trigger rock falls and dry granular flows, but is a very slow process. Another hypothesis is that adsorbed water, which makes grains sticky, is released at high temperatures, allowing dry mass wasting, but the association with bedrock and rocky slopes is left unexplained. Triggering by seasonally high winds or dust devils is possible, but doesn't explain the absence of RSL in the northern hemisphere or the orientation preference of the mid-latitude features. None of these hypotheses explain why RSL are abundant in rare places and absent from most steep rocky slopes; other difficulties are listed in table S5. Nevertheless, all of these hypotheses deserve further consideration.

The latitudinal preference of RSL and their fading in cold seasons suggest some role for a volatile. CO_2 sublimation drives many dynamic phenomena on Mars (*18*), but CO_2 probably never freezes on these equator-facing slopes and certainly is not present in the summer. Nearly pure H_2O, if present, might drive activity, but (i) the ice would rapidly sublimate to dry out these warm slopes, and (ii) some RSL activity occurs below the freezing point for pure water (table S1).

The definite association between RSL and temperatures greater than 250 K points to brines as the most relevant volatile. The Spirit landing site in Gusev Crater (14.6°S) reaches temperatures similar to those of the RSL slopes (table S1); the subsurface temperature at the hottest times should exceed 250 K down to at least 2 cm depth (*21*). Many brines expected on Mars have eutectic temperatures (T_e) below 250 K, except most sulfates (*2*, *10*); RSL have not been found near the extensive sulfate deposits mapped from orbit (*4*). The most likely brine compositions relevant to RSL are chlorides (Mg, Na, or Ca) or Fe sulfates, with T_e from 205 to 250 K.

Brines could lead to RSL from seeps or thin flows. The formation mechanism could resemble that of (*22*) for putative "wet" slope streaks, in which the warm-season temperature exceeds T_e at depths of a few centimeters, brines percolate and refreeze at depth to form an impermeable layer, and downslope percolation occurs at the interface between liquid and frozen brine. Alternatively, a thin debris flow might be mobilized at the liquid/ice interface. This model should be more effective over surfaces with moderate to high thermal inertias, warming a thicker layer above the brine eutectic. For either seeping or debris flow, sufficient water to fill pore spaces is needed; interfacial water (*23*) is probably not sufficient. Given the lack of water absorption bands in CRISM spectra, we assume that RSL are usually dry at the surface, perhaps wet only in the subsurface and perhaps in small surface areas while moving.

The origin of the water to form RSL could be the absorption of water vapor by hygroscopic salts (deliquescence) or subsurface seeps. Deliquescence from the atmosphere, most likely in the polar regions where relative humidity is higher, might occur in the middle latitudes (*10*), although it is unclear whether sufficient water can be trapped each year. Deliquescence might also result from sublimation of relict subsurface ice and the diffusion of water vapor toward the surface (SOM). RSL formation would be localized by concentrations of hygroscopic salts and water vapor, in addition to other factors. Salt concentrations at RSL sites have not been identified from CRISM data, but anhydrous chlorides lack distinctive absorption bands (*24*).

To produce brine seeps from groundwater, there must be sufficient liquid to fill the pore space between particles and create a hydraulic gradient to initiate and maintain water flow to the surface. Although many RSL occur in favorable topographic locations for groundwater (Fig. 2 and figs. S3 and S4), some do not (Fig. 1). Another difficulty is that the RSL-bearing slopes are too warm to preserve shallow ground ice in equilibrium with the atmosphere (*25*). RSL formation, if driven by groundwater seeps, must be a nonequilibrium process, requiring ground-

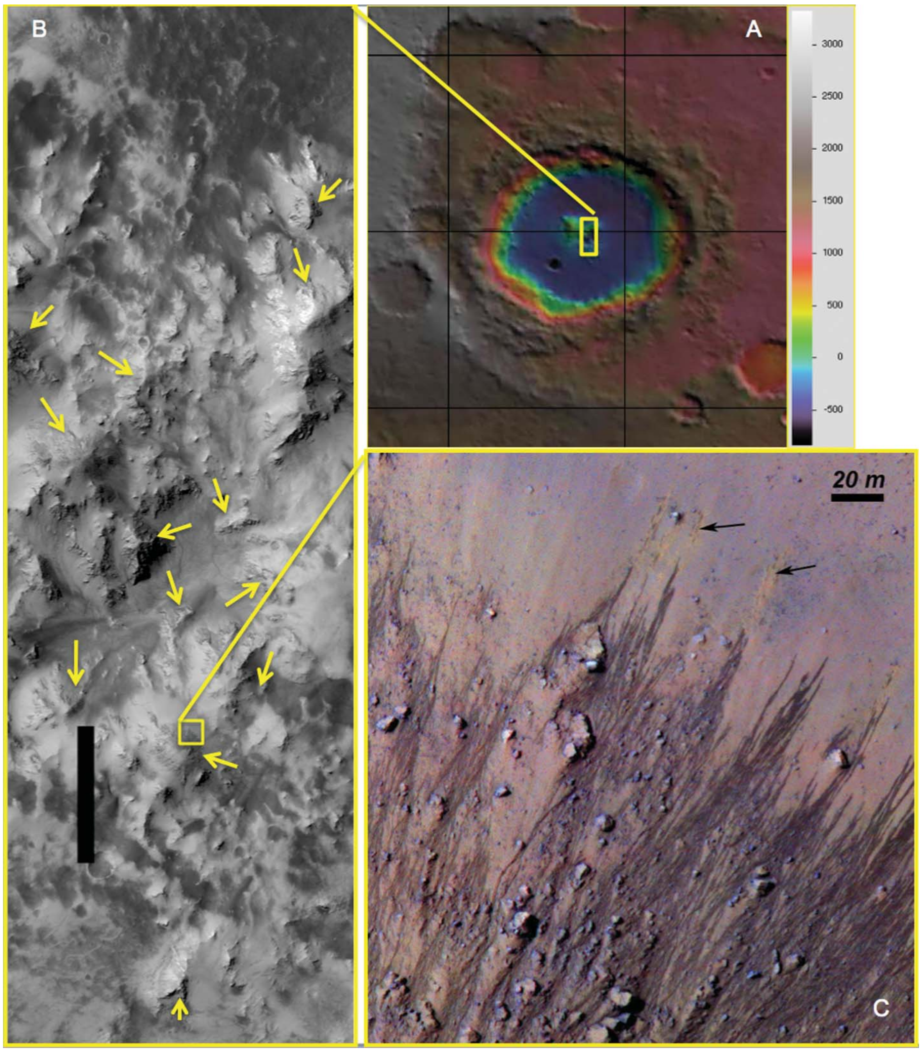

Fig. 1. RSL on the central structure of Horowitz Crater (32°S, 140.8°E), MRO Primary Science Phase (PSP) image PSP_005787_1475 (L_S = 334: late summer). Altimetry map (**A**) locates the full 5.1-km-wide HiRISE image (**B**), with the white box indicating the color enlargement (**C**). Yellow arrows in (B) show some concentrations of RSL within the central peaks and pits. Colors in (C) have been strongly enhanced to show the subtle differences, including light orange streaks (black arrows) in the upper right that may mark faded RSL. North is up on all images in this paper except fig. S4.

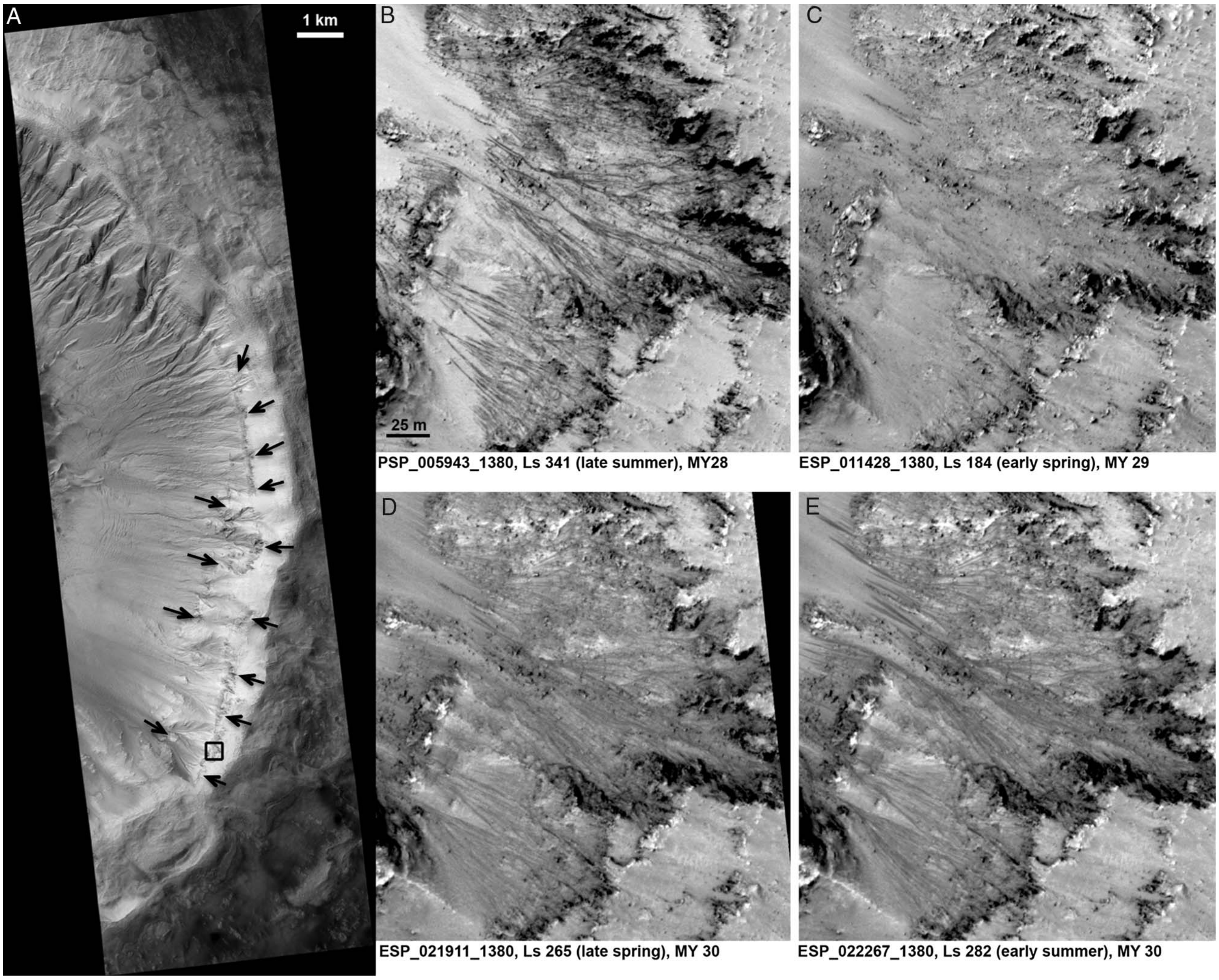

Fig. 2. Impact crater with abundant RSL at 41.6°S, 202.3°E in Newton Basin. (**A**) is the full HiRISE PSP_005943_1380; arrows point to some concentrations of RSL, and the black box locates the four blowups of orthorectified images (*13*) showing RSL (dark lines) in the late summer of MY 28 (*12*) (**B**), faded by the next very early spring (**C**), then gradually darkening and reforming in the spring (**D**) and summer (**E**) of MY 30. The RSL are located on steep north-to-west–facing slopes associated with bedrock outcrops, often in alcoves. Each image was given a minimum-maximum stretch so that shadows are black and the brightest spots are white.

water migration or active surface processes to expose subsurface brines. Modeling by (*26*) shows that groundwater discharge on Martian slopes in the present-day environment requires either (i) high permeability and ample (pure) water, (ii) geothermally heated water, or (iii) brines with a depressed freezing point. The presence of brines is the most realistic scenario for Mars, requiring modest quantities of water and no geothermal heat. Furthermore, the brine model exhibits a dependence of discharge on season and favors equator-facing slopes in the middle to high latitudes (*26*), much like the RSL.

The mechanisms of darkening and fading of RSL are uncertain. Wetting of particulate materials causes optical darkening by a combination of processes (*27*), and drying or freezing would explain the fading in cold seasons, but this model is inconsistent with the lack of water absorption bands in CRISM data. Alternatively, the RSL could darken by an increase in grain size or roughness from seeping or flows, but the fading in cold seasons still needs an explanation. The gradual settling of atmospheric dust is not a likely mechanism for the fading, based on the longer fading time scale (years, not months) of other relatively dark transient features such as slope streaks and new impact markings. Also, removal of dust during RSL formation would cause a strong color change that is not observed (SOM). RSL surface structure might change in cold seasons by a mechanism not currently understood.

We have not found any candidate RSL in the northern mid-latitudes. This may be explained by the current seasonal asymmetry, by differences in bedrock geology, or both. The putative chloride deposits, hypothesized to result from the ponding of surface runoff or groundwater upwelling, are strongly concentrated in low-albedo regions of the southern hemisphere (*24*), similar to the distribution of RSL. Brines forming the chloride deposits might infiltrate or remain underground and could be stable over geologic time in the middle latitudes in a liquid or frozen state, until new craters or troughs expose the brines on warm slopes. This could explain the association of RSL with bedrock layers, either because they control the subsurface migration of fluids or water vapor or because they contain hygroscopic salt-rich lenses such as buried chloride deposits.

Liquid water on Mars today would be of great interest for astrobiology. Its presence has been suggested previously. Water flow is one hypothesis for the formation of the active mid-latitude gullies (*28*), although recent observations show that gullies are active in the winter and in places where seasonal CO_2 is present and water is least likely (*29*, *30*). Briny flows have been suggested (*17*) for high-latitude dune streaks that appear during CO_2 defrosting, but CO_2 is the more likely driving volatile (*18*). Brines have been suggested for slope streaks (*22*), but there is no

Table 2. Slope streaks versus RSL.

Attribute	Slope streaks	RSL
Slope albedo	High (>0.25)	Low (<0.2)
Contrast	~10% darker	Up to 40% darker
Dust index*	High (e < 0.95)	Low (e > 0.96)
Thermal inertia	Low (<100)	180 to 340
Width	Up to 200 m	Up to 5 m
Slope aspect preferences	Varies with regional wind flow (*15*)	Equator-facing in middle latitudes
Latitudes; longitudes	Corresponds to dust distribution	32°S to 48°S; all longitudes
Formation L_S	All seasons (*31*)	L_S = 240 to 20
Fading time scale	Years to decades	Months
Associated with rocks	No	Yes
Associated with channels	No	Yes
Abundance on a slope	Up to tens	Up to thousands
Regional mineralogy	Mars dust	Variable
Formation events	One event per streak or streaks	Incremental growth of each feature
Yearly recurrence	No	Yes

*1350 to 1400 cm^{-1} emissivity (e) (SOM).

seasonality to their formation (*31*). The Phoenix lander may have observed droplets of brine on the lander legs (*9*), and perchlorates should form liquids at times (*8*, *32*), but definitive evidence for liquid at the landing site is lacking (*33*).

References and Notes

1. B. C. Clark, *Icarus* **34**, 645 (1978).
2. G. W. Brass, *Icarus* **42**, 20 (1980).
3. S. W. Squyres *et al.*, *Science* **306**, 1709 (2004).
4. A. Gendrin *et al.*, *Science* **307**, 1587 (2005).
5. M. H. Hecht *et al.*, *Science* **325**, 64 (2009).
6. D. W. G. Sears, J. D. Chittenden, *Geophys. Res. Lett.* **32**, L23203 (2005).
7. T. Altheide, V. Chevrier, C. Nicholson, J. Denson, *Earth Planet. Sci. Lett.* **282**, 69 (2009).
8. M.-P. Zorzano, E. Mateo-Marti, O. Prieto-Ballesteros, S. Osuna, N. Renno, *Geophys. Res. Lett.* **36**, L20201 (2009).
9. N. O. Rennó *et al.*, *J. Geophys. Res.* **114**, E00E03 (2009).
10. D. Möhlmann, K. Thomsen, *Icarus* **212**, 123 (2011).
11. A. S. McEwen *et al.*, *Icarus* **205**, 2 (2010).
12. L_S is the true anomaly of Mars in its orbit around the Sun, measured from the vernal equinox, used as a measure of the season on Mars. L_S = 0 corresponds to the beginning of northern spring; L_S = 180 is the beginning of southern spring. The numbering of Mars years (MYs) was defined to facilitate comparison of data sets across decades and multiple Mars missions; year 1 started on 11 April 1955.
13. Time sequences in animated GIF format are posted at http://hirise.lpl.arizona.edu/sim/. These are stacked cutouts from orthorectified HiRISE images archived (or to be archived within 1 year) in the Planetary Data System.
14. S. L. Murchie *et al.*, *J. Geophys. Res.* **112**, E05S03 (2007).
15. J. J. Wray, S. L. Murchie, S. W. Squyres, F. P. Seelos, L. L. Tornabene, *Geology* **37**, 1043 (2009).
16. D. Baratoux *et al.*, *Icarus* **183**, 30 (2006).
17. A. Kereszturi *et al.*, *Icarus* **207**, 149 (2010).
18. C. J. Hansen *et al.*, *Science* **331**, 575 (2011).
19. P. R. Christensen *et al.*, *Space Sci. Rev.* **110**, 85 (2004).
20. H. Viles *et al.*, *Geophys. Res. Lett.* **37**, L18201 (2010).
21. R. Ulrich, T. Kral, V. Chevrier, R. Pilgrim, L. Roe, *Astrobiology* **10**, 643 (2010).
22. M. Kreslavsky, J. W. Head, *Icarus* **201**, 517 (2009).
23. K. J. Kossacki, W. J. Markiewicz, *Icarus* **210**, 83 (2010).
24. M. M. Osterloo, F. S. Anderson, V. E. Hamilton, B. M. Hynek, *J. Geophys. Res.* **115**, E10012 (2010).
25. M. T. Mellon, W. C. Feldman, T. H. Prettyman, *Icarus* **169**, 324 (2004).
26. J. M. Goldspiel, S. W. Squyres, *Icarus* **211**, 238 (2011).
27. H. Zhang, K. J. Voss, *Appl. Opt.* **45**, 8753 (2006).
28. M. C. Malin, K. S. Edgett, L. V. Posiolova, S. M. McColley, E. Z. Dobrea, *Science* **314**, 1573 (2006).
29. C. M. Dundas, A. S. McEwen, S. Diniega, S. Byrne, S. Martinez-Alonso, *Geophys. Res. Lett.* **37**, L07202 (2010).
30. S. Diniega, S. Byrne, N. T. Bridges, C. M. Dundas, A. S. McEwen, *Geology* **38**, 1047 (2010).
31. C. M. King, N. Schorghofer, K. L. Wagstaff, *Lunar Planet. Sci. Conf.* **41**, 1542 (2010).
32. S. C. Cull *et al.*, *Geophys. Res. Lett.* **37**, L22203 (2010).
33. C. R. Stoker *et al.*, *J. Geophys. Res.* **115**, E00E20 (2010).

Acknowledgments: This research was supported by NASA's MRO project; we thank them along with the reviewers. All original data reported in this paper are tabulated in the SOM and archived by NASA's Planetary Data System.

Supporting Online Material

www.sciencemag.org/cgi/content/full/333/6043/740/DC1
SOM Text
Figs. S1 to S6
Tables S1 to S5
References (*34–48*)

25 February 2011; accepted 17 June 2011
10.1126/science.1204816

Reduced Interannual Rainfall Variability in East Africa During the Last Ice Age

Christian Wolff,[1,2,3] Gerald H. Haug,[3,4*] Axel Timmermann,[5] Jaap S. Sinninghe Damsté,[6,7] Achim Brauer,[1] Daniel M. Sigman,[8] Mark A. Cane,[9] Dirk Verschuren[10]

Interannual rainfall variations in equatorial East Africa are tightly linked to the El Niño Southern Oscillation (ENSO), with more rain and flooding during El Niño and droughts in La Niña years, both having severe impacts on human habitation and food security. Here we report evidence from an annually laminated lake sediment record from southeastern Kenya for interannual to centennial-scale changes in ENSO-related rainfall variability during the last three millennia and for reductions in both the mean rate and the variability of rainfall in East Africa during the Last Glacial period. Climate model simulations support forward extrapolation from these lake sediment data that future warming will intensify the interannual variability of East Africa's rainfall.

In the tropics, changes in rainfall patterns have severe consequences for millions of people. East Africa, in particular, has in recent years experienced both extreme flooding and severe droughts, with serious impacts on developing economies and wildlife throughout the region (*1*). Seasonality in East African climate is controlled primarily by the biannual migration of the Intertropical Convergence Zone (ITCZ) across the region (*2*) (fig. S1). As a result, equatorial East Africa experiences two climatological rainy seasons (*3*). Dry seasons are windy because of the trade winds that straddle the ITCZ. Interannual variations in the seasonal migration of the East African ITCZ are driven to a large extent by the El Niño Southern Oscillation (ENSO) (*4*) and its related western Indian Ocean sea surface temperature (SST) anomalies (*5*, *6*). El Niño events alter the atmospheric circulation, often generating an equatorial Indian Ocean SST pattern that is warmer in the west and cooler in the east, a configuration sometimes referred to as the positive phase of the Indian Ocean Dipole Mode (*7*). Surface ocean warming in the western Indian Ocean leads to intensification and shifts of the ITCZ, bringing more precipitation to East Africa and weakening the local surface winds (*8*, *9*) (Fig. 1A). El Niño thus tends to enhance East African rainfall indirectly